Biol Trace Elem Res (2017) 178:98–104
DOI 10.1007/s12011-016-0892-z

Nickel Oxide Nanoparticles Induce Oxidative DNA Damage and Apoptosis in Kidney Cell Line (NRK-52E)

Mahmoud Abudayyak[1] · **Elif Guzel**[2] · **Gül Özhan**[1]

Received: 13 August 2016 / Accepted: 7 November 2016 / Published online: 22 November 2016

Abstract Increasing use of nickel oxide (NiO) nanoparticles in different applications results in high occupational and environmental exposure to them. However, the effect of NiO nanoparticles on human health is still poorly documented. It was aimed to investigate the toxic potentials of NiO nanoparticles on NRK-52E kidney epithelial cells. The following assays were used: the nanoparticle characterization by transmission electron microscopy (TEM) and dynamic light scattering (DLS); the determination of cellular uptake and morphologic changes by TEM and inductively coupled plasma-mass spectrometry (ICP-MS); MTT and neutral red uptake (NRU) assays for cytotoxicity; comet assay for genotoxicity; the determination of malondialdehyde (MDA), 8-hydroxydeoxyguanosine (8-OHdG), protein carbonyl (PC) and glutathione (GSH) levels by enzyme-linked immune sorbent assays (ELISA) for the potential of oxidative damage; and Annexin V-FITC apoptosis detection assay with propidium iodide (PI) for apoptosis. The nanoparticles were taken up by the cells and induced dose-dependent DNA damage by comet assay and oxidative damage evidenced by increasing levels of MDA, 8-OHdG, PC and depletion of GSH. At ≥294.0 μg/mL concentration, NiO nanoparticles caused 50% inhibition in cell viability by the cytotoxicity assays. Also, they showed apoptotic/necrotic effects on the cells as well as some morphological changes. We have indicated that their cellular damage effects should raise concern about the safety associated with their applications in consumer products.

Keywords Nickel oxide nanoparticles · Nephrotoxicity · Genotoxicity · Oxidative stress · Apoptosis

Introduction

Nickel oxide (NiO) nanoparticles are important industrial nanomaterials and widely used as catalysts, electrochromic materials and sensor and colouring agents. Battery manufacturing, printing, solar cells, lithium-ion batteries, light-emitting diodes, electrochemical sensors and biosensors are some of the technological applications of NiO nanoparticles [1, 2]. Occupational exposure to nickel-based nanoparticles can occur through the production of metal alloys, batteries, paints etc. in addition to environmental exposure occurring mainly through industrial products being released and then settling in soil, water resources and food supplies [3]. Environmental exposure was observed with nickel lead to atmospheric concentrations in suburban areas from 6 to 17 ng/m^3 and in industrialized areas from 120 to 170 ng/m^3 [3]. It was reported approximately 2% of the work force in nickel-related industries have been exposed to airborne nickel-containing particles in concentrations ranging from 0.1 to 1 mg/m^3 [4].

Nickel compounds including NiO are classified as class 1 carcinogenic materials by the International Agency for Research on Cancer (IARC) [5]. Generally, toxic effects of NiO nanoparticles have mainly been investigated for airway cells in mammalian systems and found to induce oxidative stress and inflammatory responses related to lung toxicity [6–11]. Compared with fine particles of NiO (~1 μm), NiO nanoparticles released a high amount of Ni^{+2} into a culture

✉ Gül Özhan
gulozhan@istanbul.edu.tr

[1] Faculty of Pharmacy, Department of Pharmaceutical Toxicology, Istanbul University, Beyazit, 34116 Istanbul, Turkey

[2] Cerrahpasa Medical Faculty, Department of Histology and Embryology, Istanbul University, Fatih, 34098 Istanbul, Turkey

medium [1]. NiO nanoparticles showed strong cytotoxicity via cellular uptake and induced oxidative stress both with direct effect and with reactive oxygen species produced by phagocytes such as macrophages and neutrophils [1, 7, 12]. Internalized nanoparticles can result in extended exposure depending on nanoparticle retention. Differences in size and shape of nanoparticles might change their retention time and their toxic effects [13]. Indeed, Ispas et al. [13] observed that the nickel nanoparticles were equal to or less toxic than were soluble nickel while dendritic clusters were more toxic when they exposed three different-size nickel nanoparticles (30, 60 and 100 nm) and larger particle clusters of aggregated 60-nm entities with a dendritic structure to zebrafish embryos and compared the results to soluble nickel salts.

NiO nanoparticles are absorbed as they pass through the gastrointestinal tract and are distributed to different organs like the liver via the circulatory system [11, 14, 15]. In the NiO inhalation exposure study conducted by Tanaka et al., it was reported that nickel was found in the liver and kidneys after inhalation, which indicated the delivery of nickel to those organs [16]. Choi et al. [17] reported differential retention in kidneys was observed due to the size and shape of nanoparticles. Small spherical nanoparticles were cleared from rat kidney, while larger nanoparticles were not excreted [17]. In a 38-year-old previously healthy male, inhaled nickel nanoparticles while spraying nickel onto bushes for turbine bearings using a metal arc process was re-examined by Philip et al. [18] from a pathology perspective. Nickel nanoparticles (<25 nm) were identified in lung macrophages, and high levels of nickel were measured in his urine and kidneys, which showed evidence of acute tubular necrosis, although the cause of his death was adult respiratory distress syndrome.

There has been no study yet related to the toxicological assessment of NiO nanoparticles in kidney. The present study aimed to investigate their toxic effects on NRK-52E kidney epithelial cell by various toxicological endpoints, including cytotoxicity, genotoxicity, oxidative damage, apoptosis and cellular morphological changes, following the evaluation of the size and cellular uptake of the nanoparticles in vitro.

Materials and Methods

Cell culture medium (Dulbecco's modified Eagle's medium (DMEM) F-12), phosphate buffer solution (PBS) and all other supplements were purchased from Multicell Wisent (Quebec, Canada). GSH, 8-OHdG, MDA and PC ELISA kits were purchased from Yehua Biological Technology (Shanghai, China). AV-FITC apoptosis detection with PI and protein assay dye reagent was obtained from Biolegend (CA, USA) and Bio-rad (Munich, Germany), respectively. NiO nanoparticles (cat. no. 637130) and the other chemicals were obtained from Sigma (USA). NRK-52E rat kidney proximal tubular epithelial cell (CRL-1571) was purchased from American Type Culture Collection (ATCC) (MD, USA).

NRK-52E cells were incubated in DMEM-F12 medium supplemented with FBS and antibiotic/antimicotic solutions at 5% CO_2, 90% humidity and 37 °C for 24 h (60–80% confluence). The cell densities were in the range of $1 \times 10^{5-7}$ cells/mL for all assays. NiO nanoparticles were suspended at a concentration of 1 mg/mL in cell culture medium and sonicated at room temperature for 5 min to avoid the aggregation/agglomeration of the particles before exposure.

For Exposure The cells were exposed to final concentrations of 0–500 μg/mL in the cytotoxicity assays, 0–120 μg/mL in the comet assay, 0–300 μg/mL in the apoptosis/necrosis assay, 0–150 μg/mL in the oxidative damage assays, 50 and 100 μg/mL in the cellular uptake assay by ICP-MS and 50 and 150 μg/mL in the morphology examination and cellular uptake by TEM. The exposure time was 24 h.

For Particle Size Characterization NiO nanoparticles suspended in both Milli-Q water and cell culture medium were sonicated for 15 min and then dropped on carbon-coated 200-mesh cupper grid and allowed to dry prior to measurement via TEM (Jem-2100 HR, Jeol, USA). The average hydrodynamic size of NiO nanoparticles in the cell culture medium was determined by dynamic light scattering (DLS) (ZetaSizer Nano-ZS, Malvern Instruments, Malvern, UK), For this, 1 mg NiO nanoparticles was dispersed in the cell culture medium, the suspension was sonicated using a sonicator bath at room temperature for 15 min at 40 W; 10 μl of the suspension was diluted with cell culture medium to reach final concentration 10 μg/mL, sonicated for further 5 min and the DLS experiments performed.

For Cellular Uptake and Morphological Change Nickel release from the NiO nanoparticles into the cell culture medium and particle uptake from the cells were determined using the inductively coupled plasma-mass spectrometry (ICP-MS) (Thermo Elemental X series 2, USA) method. To evaluate the ion release, 200 μg/mL NiO nanoparticles were suspended in a 10-mL cell culture medium with 10% FBS and sonicated for 15 min. The NiO nanoparticle suspension was incubated at 37 °C, 5% CO_2 and 90% humidity, the exposure condition similar to the cells, for 24 h. After the medium was centrifuged at 20.000*g* for 20 min, 1 mL of the supernatant was acidified with nitric acid (65%) and incubated at room temperature for 1 h and were then stored at −20 C° until analysis. The released amount of nickel was analysed by ICP-MS. Nickel content of the cell culture medium was also measured.

Morphological change was also investigated by TEM. The cells were fixed in glutaraldehyde in Millonig's sodium phosphate buffer (pH 7.4) for 2 h at room temperature. After being washed with the buffer and centrifuged at 1200 rpm for

10 min, the cells were post-fixed in 1% osmium tetroxide in Millonig's buffer (pH 7.4) for 30 min at room temperature. Then, the cells were blocked in 2% agarose gel and dehydrated in a graded series of ethanol to absolute ethanol in preparation for embedding in araldite. Semi-thin sections from the polymerized blocks were stained with toluidine blue. Ultra-thin sections (50–60 nm) were cut by an ultramicrotome (Reichert UM 3, Austria), placed on copper grids and stained with uranyl acetate and lead citrate. Sections were analysed and photographed using a TEM (Jeol-1011, Tokyo, Japan) with attached digital camera (Olympus-Veleta TEM Camera, Tokyo, Japan).

For Cell Death Potential MTT and NRU cytotoxicity assays based on different cellular mechanisms depending on the damaged region were used [19, 20]. Optical densities (ODs) were 590 and 540 nm for MTT and NRU, respectively. The inhibition of enzyme activity observed in cells was calculated and compared to that of the unexposed (negative control) cells. Then, the half maximal inhibitory concentration (IC_{50}) values were expressed as the sample concentration that caused an inhibition of 50% in enzyme activities in cells.

For Genotoxic Potential Comet assay was used. Hydrogen peroxide (H_2O_2) (100 μM) and PBS were used as positive and negative controls, respectively. The number of DNA breaks was scored under a fluorescent microscope (Olympus BX53, Olympus, Tokyo, Japan) at ×400 magnification using an automated image analysis system (Perceptive software, Kansas, USA). DNA damage to individual cells was expressed as a percentage of DNA in the comet tail (tail intensity %) [21].

For Oxidative Damage Effects The different endpoints were measured by ELISA kits according to the manufacturer's instructions. The assays are based on biotin double antibody sandwich technology to assay human GSH, MDA, 8-OHdG or PC. The OD value was read at 450 nm using a microplate spectrophotometer system (Epoch, Germany). In every assay, the unexposed cells were evaluated as a negative control. The protein amount in 10^6 cells was measured according to Bradford dye-binding method [22], and then the protein amount was calculated for 4×10^4 cells. Results were expressed as μmol, μmol, μg and μg per g protein for GSH, MDA, 8-OHdG and PC, respectively, using standard calibration curves.

For Cellular Apoptosis or Necrosis Annexin V-FITC apoptosis detection kit with PI was used. The kit is based on observation of the translocation of the membrane

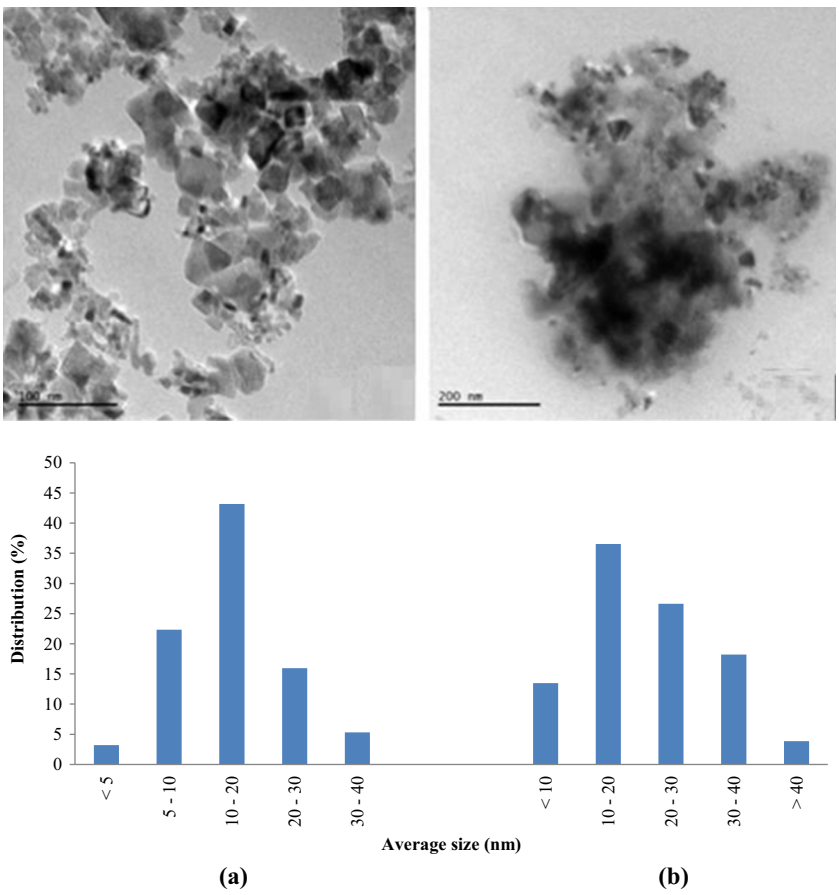

Fig. 1 TEM images of NiO nanoparticles after dissolution in water (**a**) and cell culture medium (**b**)

phosphatidylserine from the inner side of the plasma membrane to the cell surface, which can be easily detected by staining with Annexin V-FITC fluorescent dye, a protein that has a high affinity for phosphatidylserine, conjugated to FITC. Necrotic cells were labelled only with red-fluorescent PI. The exposure concentrations were chosen according to the levels that decrease the cell viability approximately in the percentage of 10, 25 and 50. In every assay, the unexposed cells were evaluated as a negative control. The apoptotic or necrotic cells distributed on the slides were immediately counted under a phase-contrast fluorescent microscope (Olympus BX53, Olympus, Tokyo, Japan). The results were expressed as the percent of the total cell amount.

For Statistical Analysis All experiments were done in triplicates and each assay was repeated four times. Data was expressed as mean ± standard deviation (SD). The significance between differences observed in the unexposed and exposed cells to the NiO nanoparticles was calculated by one-way ANOVA Dunnett *t* test using SPSS version 17.0 for Windows (SPSS Inc., Chicago, IL). *p* values less than 0.05 were selected as the levels of significance.

Results and Discussion

We aimed to evaluate NiO nanoparticle toxicities in NRK-52E cells due to that there is no study about their toxicity profiles on kidneys. For that, the particles were firstly characterized. By TEM view and DLS, the average size of the NiO nanoparticles by TEM was found to be 15.0 nm (range 4.2–38.1 nm) (Fig. 1). It was realized that the particles were slightly agglomerated or aggregated when dispersed in the cell culture medium, in which their average size was increased to 21.4 nm. According to the manufacturer, the particles that were cubic in shape had a primary particle size of ≤50 nm and purity of 99.8% and the result of X-ray diffraction conforms to the structure (Fig. 2). The DLS determination of the average hydrodynamic size of the NiO nanoparticles in the cell culture medium shows that for the NiO nanoparticles, it was 135.81 nm (ranging from 7.70 to 194.1 nm) and 33% of the particles had a size smaller than 24.8 nm.

The nickel ion release from the NiO nanoparticles was evaluated by the ICP-MS method. The cell culture medium was free of nickel ions and that no nickel ions were observed. The concentration of nickel ion was 24.90 ± 1.72 μg/mL in the cell culture NiO nanoparticle suspension, which represents 12.45% of the incubated nanoparticles. Based on that, the observed toxicological endpoints and morphological changes were mainly due to NiO nanoparticles. ICP-MS results revealed that the NiO nanoparticles were taken up by the

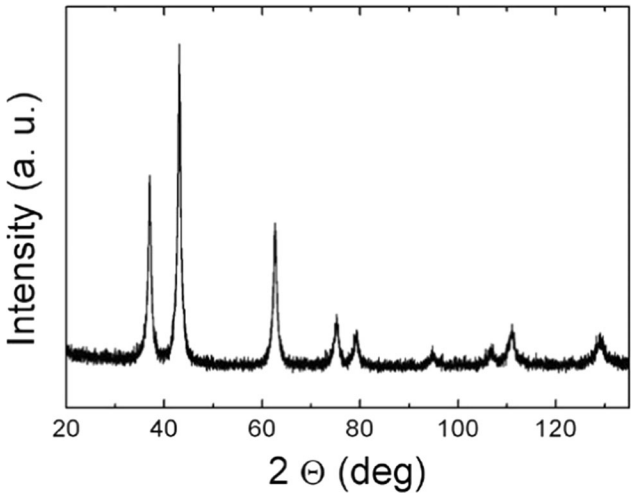

Fig. 2 The X-ray diffraction analysis of NiO-nanoparticles

NRK-52E cells in the range of 3.1–4.20 μg/10^5 cells after exposure at 50 and 100 μg/mL concentrations of the NiO nanoparticles for 24 h (Table 1). The decrease observed in the cellular uptake at high concentration could result from the agglomeration and aggregation of the particles and might be the increase in the size of NiO nanoparticles in the cell medium. Horie et al. [1] revealed the uptake of NiO nanoparticles into HaCaT human keratinocytes. Capasso et al. [23] also reported the uptake of NiO nanoparticles by A549 and BEAS-2B cells.

Cell morphology was revealed by TEM micrographs in the exposed cells to NiO nanoparticles at 50 and 150 μg/mL and in unexposed cells (Fig. 3). The nanoparticles were detected in the cytoplasmic vacuoles of NRK-52E cells, but in a few cells exposed to the particles at 50 μg/mL, they were located in the nucleus. As it is known, being smaller than cellular organelles and cells, it allows nanoparticles to penetrate basic biological structures, which may disrupt their normal function [24]. On the other hand, insoluble nickel particles are taken up by phagocytosis and dissolved in a vacuole [8]. Numerous electron-lucent and electron-dense vacuoles were observed, and mitochondria were not visible in the cytoplasm of the cells after exposure to the particles when compared with the

Table 1 Evaluation of the cellular uptakes of NiO nanoparticles by ICP-MS

Exposure concentration (μg/mL/10^5 cells)	Ni amount (μg/10^5 cells)
Negative control	0.06 ± 0.002
50	4.20 ± 0.09
100	3.10 ± 0.18

Ni content of the unexposed cells (negative control) and the exposed cells were measured. Every assay was repeated four times

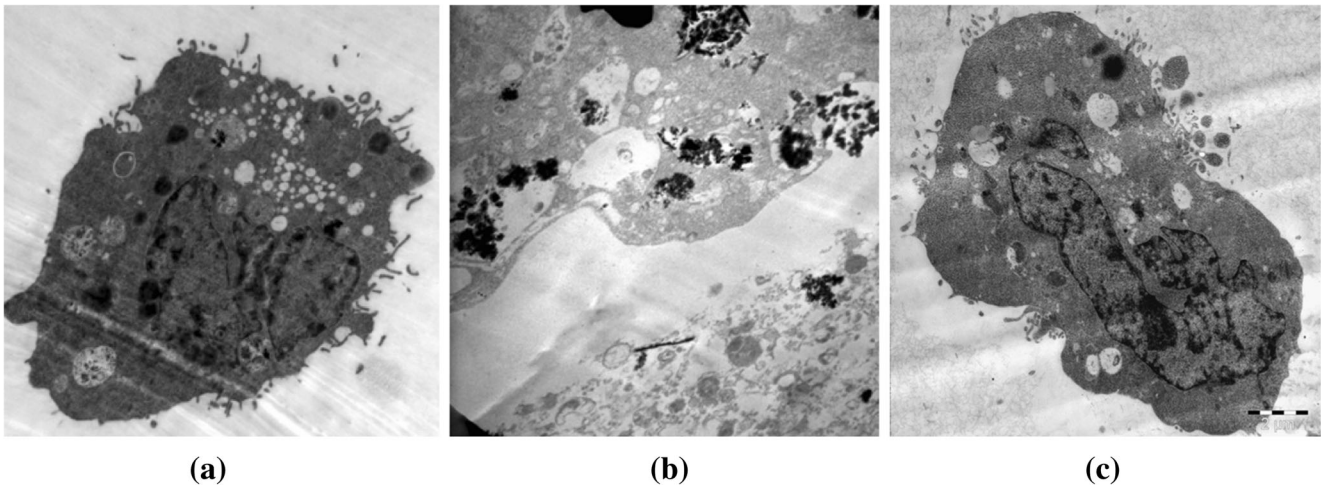

Fig. 3 TEM observations of cells after exposure to NiO nanoparticles for 24 h. **a** NRK-52E cells exposed to NiO-NPs at 50 μg/mL, **b** NRK-52E cells exposed to NiO-NPs at 150 μg/mL, **c** NRK-52E unexposed cell (negative control)

negative control cells. Electron-lucent vacuoles were noted to contain either nanoparticles or myelin figures, suggesting that they were phagosome-like structures. Most of the cells at 50 μg/mL exhibited fragmentation of the nuclei, but both the nuclear and plasma membranes appeared to be intact. The nucleus completely disappeared in some of the cells exposed to a low dose of NiO nanoparticles. After exposure to particles at 150 μg/mL, complete disruption of the cells and loss of the plasma membrane were noted in some cells. The findings suggest an apoptotic inclination in the NRK-52E kidney cells exposed to NiO nanoparticles, which turned into necrosis with increasing concentration of the particles (Fig. 3).

The cytotoxicity of the nanoparticles depends on physicochemical parameters like shape, size, hydrophobicity, surface area and surface charge, as well as biological parameters such as cell type, culture and exposure conditions influence [25, 26]. Ahamed et al. [6] reported NiO nanoparticles caused cytotoxicity via reactive oxygen species at 25–100 μg/mL. In the present study, NiO nanoparticles decreased the cell metabolic activity assessed by the disruption of mitochondrial and lysosomal functions with MTT and NRU assays. The dose-dependent reduction of cell metabolic activity could be related to an increase of cell death. The IC_{50} values of the NiO nanoparticles in NRK-52E were 294.0 and 337.2 μg/mL by MTT and NRU assays, respectively (Fig. 4). Similar to our results, Ispas et al. [13] observed that the exposure of LD_{50} levels in the range of 212–404 μg/mL concentrations resulted in skeletal muscle fibre separation in zebrafish embryo exposed to nickel nanoparticles (30–100 nm). They also suggest that the toxicity of nickel nanoparticles occurred by different biological mechanisms than that of soluble nickel [13]. The genotoxic potential was investigated by comet assay in NRK-52E cells at 0–120 μg/mL of NiO nanoparticles. In positive controls (100 μM H_2O_2), the tail intensity ranged from 5.04 to 20.00% in the cells. NiO nanoparticles significantly induced

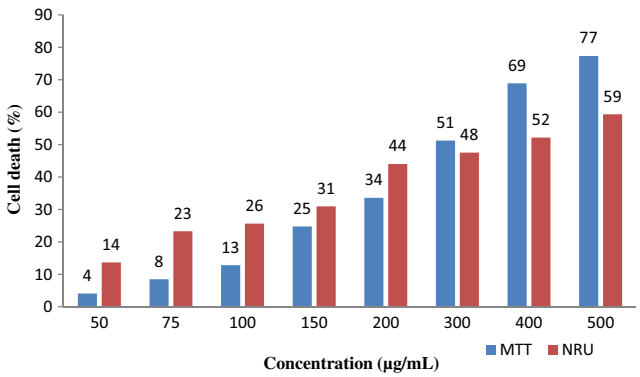

Fig. 4 Effects of the NiO nanoparticles on cell viability by MTT (**a**) and NRU (**b**). All experiments were done in triplicates and each assay as repeated four times. Data was expressed as mean

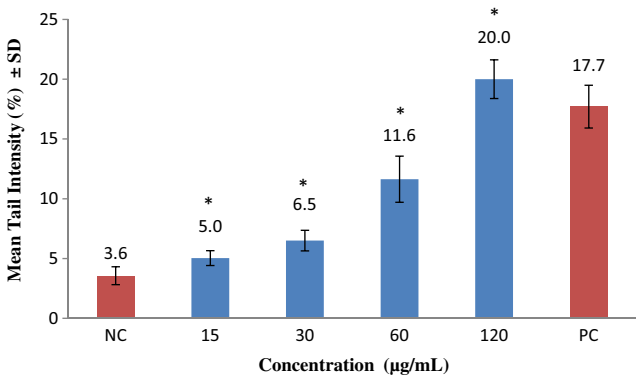

Fig. 5 Evaluation of DNA damage potentials of NiO nanoparticles assayed by comet assay. All experiments were done in triplicates and each assay was repeated four times. The results were presented as mean tail intensity (%) with ±SD. *NC* and *PC* denote mean negative and positive controls, respectively. *$p \leq 0.05$ was selected as the level of significance by one-way ANOVA Dunnett *t* test

Table 2 Evaluation of oxidative damage potentials of NiO nanoparticles in the cell lines assayed by measuring the levels of GSH, MDA, 8-OHdG and PC by ELISA

Exposure concentration (μg/mL)	8-OHdG (μg/g protein)	MDA (μmol/g protein)	GSH (μmol/g protein)	PC (μg/g protein)
0	0.972 ± 0.012	0.323 ± 0.010	41.299 ± 1.230	5.166 ± 0.435
50	0.957 ± 0.034	0.336 ± 0.006	28.050 ± 0.967*	5.487 ± 0.421
75	1.042 ± 0.023	0.397 ± 0.009	36.638 ± 1.028*	5.550 ± 0.278*
100	1.099 ± 0.041	0.397 ± 0.012	36.569 ± 0.847*	6.564 ± 0.634*
150	1.081 ± 0.025	0.424 ± 0.006*	40.211 ± 1.312	6.770 ± 0.591*

All experiments were done in triplicates and each assay as repeated four times. Data was expressed as mean ± SD

*$p \leq 0.05$ was selected as the level of significance by one-way ANOVA Dunnett t test

DNA damage in NRK-52E (1.4–5.6-fold), depending on the concentration ($p \leq 0.05$). At their highest concentration (120 μg/mL), the cell death was ≤10% (Fig. 5).

The reaction of nanoparticles with cell membranes results in ROS generation, and then oxidative stress, which leads to breakdown of membrane lipids, imbalance of intracellular calcium homeostasis, alterations in metabolic pathways and apoptosis [27, 28]. The oxidative potential of NiO nanoparticles was described earlier for HepG2, human lung carcinoma (A549) and human airway epithelial (HEp-2) and human breast epithelial (MCF-7) cells at 2–100 μg/mL [6, 11, 15]. Similarly, it was observed that NiO nanoparticles induced oxidative damage in NRK-52E cells by increasing the levels of MDA and PC and decreasing the GSH levels at concentrations of 50–150 μg/mL. An increase in the levels of MDA (≤1.3-fold) and PC (≤1.3-fold) was observed while a decrease was observed in the GSH levels (≤32.1%). However, the 8-OHdG levels, which are a biomarker of DNA oxidative damage, did not change. PC levels increased significantly at ≥75 μg/mL while GSH depletion was significant in the range of 50–100 μg/mL ($p \leq 0.05$) (Table 2).

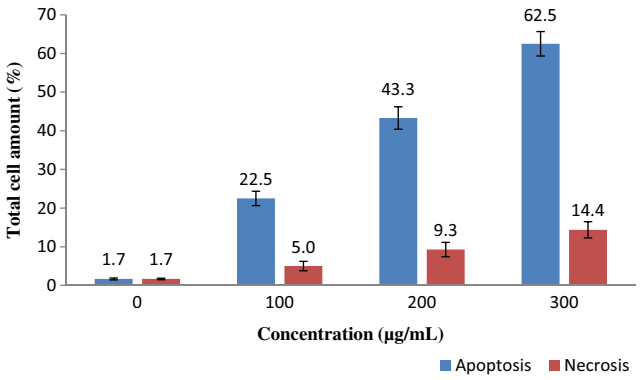

Fig. 6 Evaluation on the apoptosis- and necrosis-inducing potentials of NiO nanoparticles assayed by Annexin V-FITC-PI apoptosis detection assay. The results were presented as percentage of the total cell amount. All experiments were done in triplicates and each assay was repeated four times

Ahamed et al. [6] indicated that NiO nanoparticles caused a significant increase in micronuclei induction in HepG2 liver cells. They found that the expressions of mRNA levels of apoptotic genes bax and caspase-3 were up-regulated, whereas expression of anti-apoptotic gene bcl-2 was down-regulated in HepG2 cells. Siddiqui et al. [11] reported that NiO nanoparticles induced cytotoxicity, oxidative stress and apoptosis with increasing caspase-3 enzyme activity and DNA fragmentation in HEp-2 and MCF-7 cells in a dose-dependent manner at 2–100 μg/mL. NiO nanoparticles induced apoptosis triggered by alteration of mitochondrial and lysosome functions at 25–100 μg/mL in HepG2 cells [10]. Phillips et al. [18] indicated that nickel nanoparticles (<25 nm) were identified in lung macrophages and high levels of nickel were measured in his urine in autopsy according to a healthy male subject that inhaled nickel nanoparticles while spraying nickel materials during metal process. They also reported acute tubular necrosis was observed in his kidneys. In the present study, the cell death via apoptosis or necrosis was assessed by Annexin V-FITC with PI apoptosis detection assay; our results show that apoptosis is the main cell death pathway in NRK-52E cells exposed to NiO nanoparticles, at the highest concentrations (300 μg/mL) which were equivalent to 75% of cell death, and the apoptosis was 62.5% of the total cell amount, whereas the necrosis was 14.4% at the same concentrations (Fig. 6).

In conclusion, humans are exposed to nanoparticles both directly, due to their wide range of applications, and indirectly, via the content in bulk material. Even if the nanoparticles can affect cellular molecules in the exposed organ or system, there is a serious lack of information concerning their effects on human health and the environment. NiO nanoparticles induced DNA damage, apoptosis and oxidative stress. Therefore, there should be more concern on the safety associated with their applications in consumer products. Still, supporting in vivo studies are needed to fully understand the mechanism of NiO nanoparticle toxicity. Potential hazardous effects to human health should be more carefully and thoroughly assessed in both the industrial and commercial applications of NiO nanoparticles.

Acknowledgements This work was supported by the Research Fund of Istanbul University (Project No: 37785).

Author Contributions Dr. M. Abudayyak carried out the cell culture and exposure conditions, the toxicological assays and the particle characterization. Prof. Dr. G. Özhan participated in the toxicological assays and carried out the evaluation of the results. Dr. E. Guzel carried out the uptake and morphological changes in the cells.

Compliance with Ethical Standards

Conflict of Interest The authors declare that they have no conflict of interest.

References

1. Horie M, Nishio K, Fujita K et al (2009) Ultrafine NiO particles induce cytotoxicity in vitro by cellular uptake and subsequent Ni(II) release. Chem Res Toxicol 22:1415–1426
2. Morimoto Y, Hirohashi M, Ogami A et al (2011) Pulmonary toxicity following an intratracheal instillation of nickel oxide nanoparticle agglomerates. J Occup Health 53:293–295
3. Patel E, Lynch C, Ruff V et al (2012) Co-exposure to nickel and cobalt chloride enhances cytotoxicity and oxidative stress in human lung epithelial cells. Toxicol Appl Pharmacol 258: 367–375
4. Denkhaus E, Salnikow K (2002) Nickel essentiality, toxicity, and carcinogenicity. Crit Rev Oncol Hematol 42:35–56
5. International Agency for Research on Cancer (IARC) 1990 IARC monographs on the evaluation of carcinogenic risks to humans, volume 49, Chromium, Nickel and Welding, pp 257–445
6. Ahamed M, Ali D, Alhadlaq HA et al (2013) Nickel oxide nanoparticles exert cytotoxicity via oxidative stress and induce apoptotic response in human liver cells (HepG2). Chemosphere 93:14–22
7. Horie M, Fukui H, Nishio K et al (2011) Evaluation of acute oxidative stress induced by NiO nanoparticles in vivo and in vitro. J Occup Health 53:64–74
8. Kang GS, Gillespie PA, Gunnison A et al (2011) Comparative pulmonary toxicity of inhaled nickel nanoparticles: role of deposited dose and solubility. Inhal Toxicol 23(2):95–103
9. Lu S, Duffin R, Poland C et al (2009) Efficacy of simple short-term in vitro assays for predicting the potential of metal oxide nanoparticles to cause pulmonary inflammation. Environ Health Perspect 117:241–247
10. Nishi K, Morimoto Y, Ogami A et al (2009) Expression of cytokine-induced neutrophil chemoattractant in rat lungs by intratracheal instillation of nickel oxide nanoparticles. Inhal Toxicol 21:1030–1039
11. Siddiqui MA, Ahamed M, Ahmad J et al (2012) Nickel oxide nanoparticles induce cytotoxicity, oxidative stress and apoptosis in cultured human cells that is abrogated by the dietary antioxidant curcumin. Food Chem Toxicol 50:641–647
12. Horie M, Fukui H, Endoh S et al (2012) Comparison of acute oxidative stress on rat lung induced by nano and fine-scale, soluble and insoluble metal oxide particles: NiO and TiO_2. Inhal Toxicol 24(7):391–400
13. Ispas C, Andreescu D, Patel A et al (2009) Toxicity and developmental defects of different sizes and shape nickel nanoparticles in zebrafish. Environ Sci Technol 43:6349–6356
14. Oberdorster G, Oberdorster E, Oberdorster J (2005) Nanotoxicology: an emerging discipline evolving from studies of ultrafine particles. Environ Health Perspect 113:823–839
15. Ahmad J, Alhadlaq HA, Siddiqui MA et al (2013) Concentration-dependent induction of reactive oxygen species, cell cycle arrest and apoptosis in human liver cells after nickel nanoparticles exposure. Environ Toxicol 30:137–148
16. Tanaka I, Horie A, Haratake J et al (1988) Lung burden of green nickel oxide aerosol and histopathological findings in rats after continuous inhalation. Biol Trace Elem Res 16:19–26
17. Choi HS, Liu W, Misra P et al (2007) Renal clearance of quantum dots. Nat Biotechnol 25(10):1165–1170
18. Phillips JI, Green FY, Davies JA, Murray J (2010) Pulmonary and systemic toxicity following exposure to nickel nanoparticles. Am J Ind Med 53:763–767
19. Repetto G, del Peso A, Zurita JL (2008) Neutral red uptake assay for the estimation of cell viability/cytotoxicity. Nat Protoc 3:1125–1131
20. Van Meerloo J, Kaspers GJ, Cloos J (2011) Cell sensitivity assays: the MTT assay. Methods Mol Biol 731:237–245
21. Collins AR (2004) The comet assay for DNA damage and repair principles, applications, and limitations. Mol Biotechnol 26:249–261
22. Bradford MM (1976) A rapid and sensitive method for the quantitation of microgram quantities of protein utilizing the principle of protein-dye binding. Anal Biochem 7:248–254
23. Capasso L, Camatini M, Gualtieri M (2014) Nickel oxide nanoparticles induce inflammation and genotoxic effect in lung epithelial cells. Toxicol Lett 7(1):28–34
24. Magaye R, Zhao J (2012) Recent progress in studies of metallic nickel and nickelbased nanoparticles genotoxicity and carcinogenicity. Environ Toxicol Pharmacol 34:644–650
25. Fröhlich E (2012) The role of surface charge in cellular uptake and cytotoxicity of medical nanoparticles. Int J Nanomedicine 7:5577–5591
26. Munoz A, Costa M Elucidating the mechanisms of nickel compound uptake: a review of particulate and nano-nickel endocytosis and toxicity. Toxicol Appl Pharmacol 260:1–16
27. Clutton S (1997) The importance of oxidative stress in apoptosis. Br Med Bull 53:662–668
28. Knaapen AM, Borm PJ, Albrecht C et al (2004) Inhaled particles and lung cancer. Part a. mechanisms. Int J Cancer 109:799–809